

SEISMIC IMAGING OF THE GEOTHERMAL FIELD AT KRAFLA, ICELAND

Chuanhai Tang, Jose A. Rial, Jonathan Lees, and Eric Thompson

Department of Geological Sciences, University of North Carolina
Mitchell Hall, CB#3315
Chapel Hill, NC 27599, USA
e-mail: chhtang@email.unc.edu

ABSTRACT

During the summer of 2004 we recorded the seismicity at the Krafla geothermal field for forty days with an array of twenty PASSCAL L-28 4.5-Hz sensors. The Krafla field is located approximately 60 km East of Akureyri in northern Iceland. The array covered an area approximately 5 km N-S by 4 km E-W. The field area is located on Holocene lava flows on the Mid-Atlantic Ridge. The array recorded approximately 5 micro-earthquakes per day at a sampling rate of 500 Hz. This high sampling rate is required to exploit newly developed theories on the frequency-dependence of shear-wave splitting (SWS). During the experiment, the injection well was stopped for ten days to study the response of the subsurface crack system to changes in water pressure. SWS is an exploration method based on the analyses of polarizations and time delays of shear waves that have been distorted by the anisotropy of the medium through which the seismic waves have propagated. Epicenters roughly align along the E-W direction, while hypocenters are shallow around the injection well and appear to be related to the on-going injection. Observations of SWS at Krafla have provided evidence for at least two major crack systems oriented approximately N-S and E-W. This last, rather unexpected direction is consistent with results from a simultaneous MT (magneto-telluric) survey. Further SWS study will lead to a more detailed understanding of the fracture locations, sizes, and orientations in the geothermal field.

Keywords: shear-wave splitting, the Krafla geothermal field, seismic imaging, fractured reservoir

INTRODUCTION

The Krafla volcanic system is made up of the Krafla central volcano and an approximately 100 km long, transecting fissure swarms in northeastern Iceland. The central volcano is a major eruptive center which is less than 500, 000 years old. The Krafla central volcano is approximately 21 km long by 17 km wide

and encloses a 10 km by 7 km caldera that was formed 100,000 years ago during the last interglacial period. Two high-temperature geothermal areas occur within the Krafla volcanic system. One is located 5 km south of the Krafla caldera and the other, the NW-SE aligned Krafla-Leirhnukur geothermal field, is located inside the Krafla caldera. The eastern part of the Krafla-Leirhnukur geothermal field is utilized by the Krafla power plant which started operation in 1978. There is a shallow crustal magma reservoir with an upper boundary at a depth of approximately 3 km, near the center of inflation in the caldera (Einarsson, 1978). This magma chamber is smaller than the caldera, about 2-3 km in the N-S direction and 8-10 km in the E-W direction, with a thickness of 0.75-1.8 km (Brandsdottir et al., 1997). Geodetic measurements support the existence of a shallow magma chamber at a depth of 3 km within the caldera and have been used to argue for the existence of multiple magma reservoirs at depth (Tryggvason, 1986).

During the months of July and August 2004, a 20-station, 3-component seismic array was deployed around the Krafla geothermal field. The field area is located on Holocene lava flows on the Mid-Atlantic Ridge, and the array covered an area approximately 5 km in N-S by 4 km in E-W. Between July 5th and August 11th the array continuously recorded the seismic activity in the region surrounding the injection well K-26 located 1 km north of the power plant. The distribution of seismic stations, including both free-field and vault stations, is depicted in Figure 1. Vault stations (V) were deployed in cellars of abandoned wells. Each station in the seismic array consisted of a three-component short-period MARK4 L28 (4 Hz) seismic sensor, a data-logger or DAS (Data Acquisition System), a GPS antenna, and a 12V car battery. The data were collected continuously at a rate of 500 sps (samples per second) and recorded on 1- or 2-GB flash cards and microdisks. Stations recorded an average of 170 MB of data per day. Though the total number of functioning stations was never greater than 20, identification numbers run up to 23 because three stations had to be either moved to avoid excessive

seismic noise or entirely replaced, which required their old ID numbers to be changed.

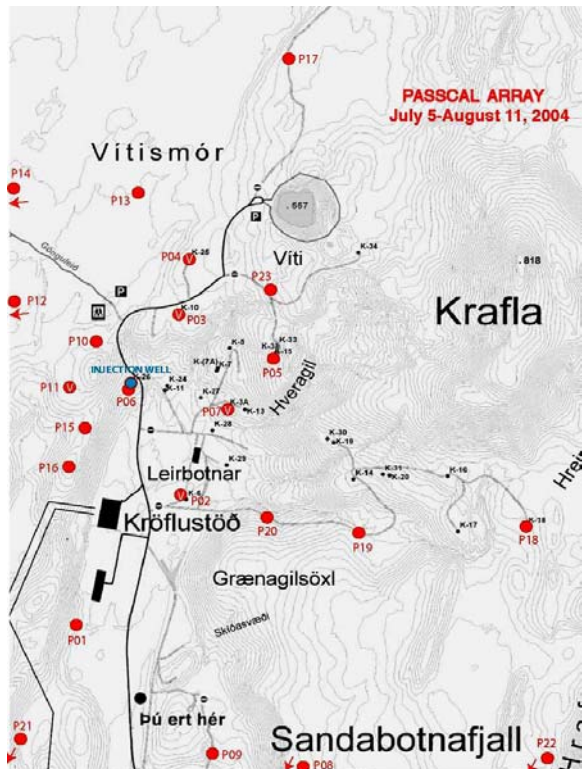


Figure 1. Distribution of the stations of PASSCAL seismic array in Krafla geothermal field, Iceland. The solid red dots represent free-field stations and the red dots with “V” are vault stations deployed in cellars of abandoned wells. The solid blue dot is where the injection well is located.

The seismic array is of the PASSCAL type, on loan from the Incorporation Research Institutions for Seismology (IRIS), which is underwritten by the US National Science Foundation. The main objective of this experiment is to use various seismic data processing techniques such as high precision earthquake location, shear-wave splitting (SWS), and tomographic inversion to detect the orientation, density and fluid content of the main subsurface fracture systems in Krafla. To further make use of the unique opportunity offered by Landsvirkjun to deploy the array, an experiment was conducted whereby injection in well K-26 was stopped on July 15th and subsequently resumed on July 26th. The response of the subsurface crack system to these transient changes in water pressure can be detected with seismic waves and will provide invaluable information on the preferred directions of fluid migration in the reservoir, permeability, effects of pore pressure on seismicity and crack activation, and three-dimensional stress variations throughout the reservoir.

OBSERVATIONS AND MEASUREMENTS OF SWS

Seismicity

Figure 2a shows the epicenters of seismic events located from July 5th to August 11th and Figure 2b shows the depth distribution of some selected events along E-W and N-S cross-sections respectively. The velocity model used in the locating is from Brandsdottir et al. (1997). Although these are preliminary locations, it is apparent that epicenters roughly align along the E-W direction, while hypocenters are shallow around the injection well. Most focal depths are shallower than 4 km.

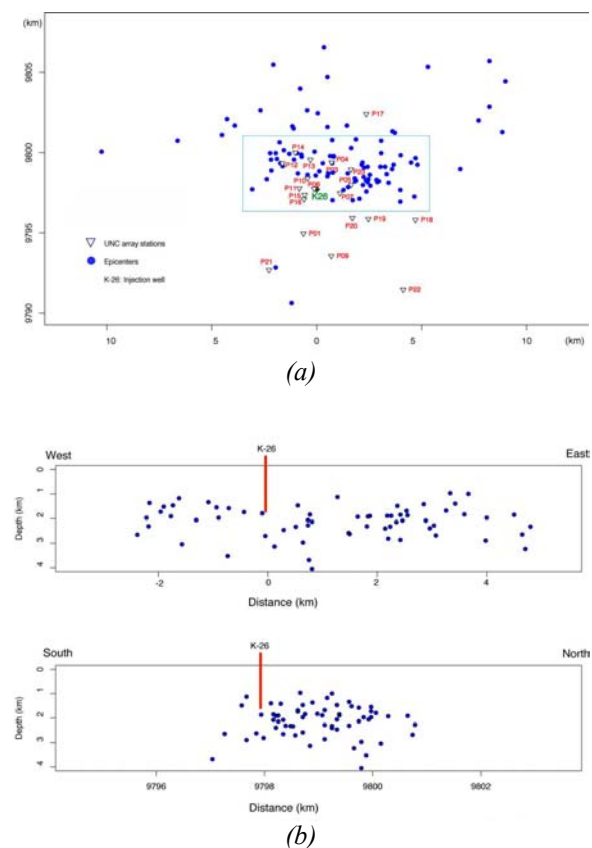


Figure 2. The seismicity recorded by UNC array from July 15th to August 11th is shown in (a). Totally 129 events are located and the depth distribution of the events located around the injection well K-26 (inside the rectangle) is shown in (b).

Seismicity at Krafla is not very high. Most events appear to be related to the on-going injection, while a few deep ones appear independent on injection. However, so far no clear relationship has emerged between injection changes and seismicity rates. During the 35 days of operations the array detected an average of 5 to 6 well-recorded events per day

(observed at 5 or more stations). These are very small earthquakes with magnitudes probably no greater than 2.

Recording seismicity at Krafla is complicated by the high level of seismic noise in the area, most of it resulting from vibrations of the steam pipes, routine plant operations, tourists, and local traffic, etc. To avoid strong sources of noise, several stations were relocated to quieter sites. Stations deployed in well cellars had a mixed performance, some noisy and some not. In spite of occasional and instrumental interruptions the UNC array performed excellently, recording over 300 GB of data in 35 days.

Shear-wave Splitting

Shear-wave splitting (SWS) is an exploration method of proven reliability and unique imaging power based on the analysis of polarizations and time delays of shear waves distorted by the anisotropic properties of the propagating medium, since no other imaging method detects both the direction and intensity of cracking. The method is based on the fact that a shear-wave propagating through rocks with stress-aligned micro-cracks (also known as *extensive dilatancy anisotropy* or EDA-cracks) will split into two waves, a fast one polarized parallel to the predominant crack direction, and a slow one, polarized perpendicular to it. The phenomenon is very similar to optical birefringence, whereby light transmitted through an anisotropic crystal undergoes analogous splitting and polarization parallel and perpendicular to the alignment of atoms in the crystal lattice. In the seismic case, the polarization direction of the fast split shear wave parallels the strike of the predominant cracks regardless of its initial polarization at the source (Crampin et al., 1986; Peacock et al., 1988). The differential time delay between the arrival of the fast and the slow shear waves (typically a few tens of milliseconds) is proportional to crack density, or number of cracks per unit volume within the rock body traversed by the seismic wave (Hudson, 1981; Crampin, 1987; Crampin and Lovell, 1991). In cracked reservoirs such as Krafla the anisotropy is likely caused by aligned systems of open, fluid-filled micro-fractures. Fortunately, the anisotropy effects on seismic waves induced by small, aligned open cracks in an otherwise isotropic rock are indistinguishable from those produced by an unfractured, but transversely isotropic medium.

Shear-wave splitting is clearly recorded in Krafla. In fact, we have recorded unusually well developed splitting that strongly points to the prevalence of at least two major crack systems oriented approximately N-S and E-W. SWS detects the predominant ~N-S fabric related to the rifting, but also provides strong evidence for an equally pervasive ~E-W lineament of

subsurface fractures roughly north and east of the injection well.

Measuring the Polarization and Time Delay

The polarization direction of the fast split shear-wave is parallel to the strike of the predominant cracks, regardless of its initial polarization at the source, and the time delay between the fast and the slow waves is proportional to the crack density. These split shear-wave properties (fast shear-wave polarization direction φ and differential time delay δt) thus constitute valuable data set to invert for the subsurface fracture geometry and to estimate the crack density and permeability anisotropy within fractured geothermal reservoirs, such as Krafla geothermal field. An important limitation to shear-wave splitting analysis is that seismic rays must be within the shear-wave window of the seismic stations. This window can be visualized as a right circular cone with vertex at the station and vertex angle $i_v = \sin^{-1}(\beta/\alpha)$, where α and β are the P- and S-wave surface velocities, respectively. For angles of incidence greater than i_v , shear waves interactive strongly with the free surface, distorting the incoming waveform (Booth and Crampin, 1985). For a half space with a typical Poisson's ratio of 0.25, the window's vertex angle, as measured from the vertical, is equal to 35°.

For the purpose of this study, we use φ and δt measurements from Krafla that correspond to high signal-to-noise ratio seismograms displaying linear horizontal particle motion and a clear well-defined shear-wave splitting event. Polarization diagrams (also known as particle motion plots) are used to accurately detect the marked switch in polarity of the two orthogonally polarized fast and slow shear-waves and to measure the split parameters (φ and δt). The polarity switch provides the clearest indication of splitting and thus of medium anisotropy. Time delays are measured after the seismogram is rotated to orient the fast and the slow waves along the instrument horizontal components. This operation cleanly decouples the two shear-wave arrivals allowing for direct and accurate measurement of the time delay. Time delays are normalized to the length of the raypath, presumed to be entirely fractured. This assumption is reasonable given that typical event depth does not exceed 4 km.

So far the data from five selected stations (P03, P04, P10, P13, and P23) have been investigated to measure the fast shear-wave polarization and time delay. These stations are selected because they either recorded the data of best quality (P13, P23) or have a relatively good coverage of raypaths coming from different azimuths (P03, P04, P10, P23). Station P13 had recorded the best data with highest signal-to-noise ratio of all the stations in the array but

unfortunately, its DAS (Data Acquisition System) was faulty and recorded no data from July 9 to 13 and was replaced with a new DAS on July 25. Station P23 was the previous P05 which was moved to the new location in order to avoid the high seismic noise there. Figure 3 shows the rose diagrams (polar histograms) of fast shear-wave polarization directions observed within the shear-wave window of the five stations. The bin size in the rose diagrams is 10° and the length of each bin is proportional to the number of polarizations within it. It can be seen from Figure 3 that the predominant polarization directions observed for stations P13 and P23 are close to E-W and those for stations P04 and P10 are close to N-S direction, while P03 shows a distinct subset of polarizations striking N-S in addition to and almost perpendicular to the main polarization set in E-W direction.

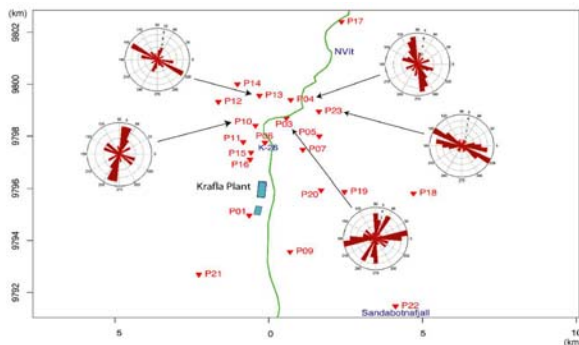


Figure 3. Rose diagrams of the fast shear-wave polarization directions observed at the five stations.

To inspect the azimuthal distribution of polarization angles, equal-area projection plot of the observed polarizations at station P13, as an example, is shown in Figure 4a. For all the five stations most shear-wave splitting events within the shear-wave window come from the NE and SE quadrants and fewest from the SW quadrant, which can be compared with the distribution of located epicenters in Figure 2a. Shown in Figure 4b is the equal-area projection plot of the observed time delays which are already normalized to the length of the corresponding raypath.

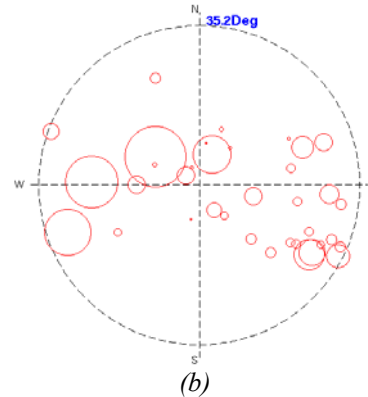
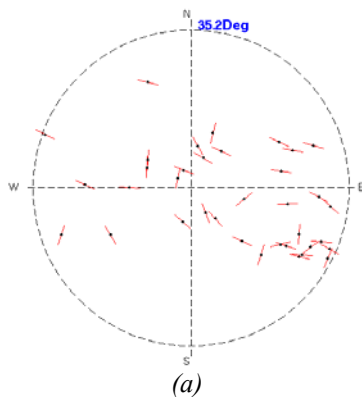


Figure 4. Observed fast shear-wave polarization angles (a) and differential time delays (b) at station P13 plotted in equal-area projection. The biggest circle corresponds to a time delay of 34 ms/km and the smallest to 1 ms/km. The shear-wave window is 35.2° .

INVERSION METHOD AND RESULTS

The pairs of anisotropy-related parameters, fast shear-wave polarization direction ϕ and differential time delay δt , read from many seismograms recorded at the five selected seismic stations at Krafla may provide a preliminary means of detecting the key subsurface fracture characteristics in the reservoir. Polarization orientations help delineate stress-aligned crack directions that represent potential conduits for subsurface fluid flow, while crack densities inferred from differential time delays may offer good prospects of depicting target-zones of increased cracking density and rock permeability within the reservoir rocks. To avoid potential ambiguity, it is worthwhile to mention that in an anisotropic medium, aligned fast shear-wave polarization orientations are independent of the initial polarization of the shear-wave at the source and are mainly caused by the medium's anisotropy (e.g. Crampin et al., 1986; Peacock et al., 1988; Crampin and Lovell, 1991).

Methodology

We use an inversion scheme employing both shear-wave splitting parameters ϕ and δt (Yang, 2003). As previously discussed, ϕ mainly depends on the angle between the crack normal and the seismic ray while δt is proportional to the crack density along the raypath. Station-by-station inversion for subsurface crack strike, dip and density is performed through successive trial-and-error comparisons of observed and theoretical fast shear-wave polarizations and associated time delays plotted in equal-area projections as functions of ray azimuth and angle of incidence. The trial-and-error process is guided, in the sense that the fit of a given crack model is interactively optimized by displaying the history of

all previous trial-and-error events, so that current results guide the next update trial until convergence to the best solution is achieved. Simultaneous minimization of both φ and δt residuals is accomplished by a non-linear least-squares algorithm whereby the goodness-of-fit of a given crack model is evaluated based on the root mean square (RMS) estimates given by

$$RMS(\varphi) = \left\{ \frac{1}{N-2} \sum_{n=1}^N ((\varphi_o)_n - (\varphi_t)_n)^2 \right\}^{1/2} \quad (1)$$

$$RMS(\delta t) = \left\{ \frac{1}{N-2} \sum_{n=1}^N ((\delta t_o)_n - (\delta t_t)_n)^2 \right\}^{1/2} \quad (2)$$

where φ_o and φ_t are observed and theoretical fast shear-wave polarization angles respectively, δt_o and δt_t are observed and theoretical differential time delays respectively, and N is the number of observations recorded at a given seismic station.

Essentially, inversion efforts are expected to identify regions of different crack densities in Krafla geothermal field and invert for 3-D fracture geometry in the subsurface. Based on seismic ray coverage and depending on the spatial patterns and azimuthal distributions of observed polarizations and time delays in the equal-area projection plots, crack-induced anisotropy is modeled by 1) a single system of vertical cracks, 2) a single system of non-vertically dipping cracks, or 3) two intersecting sets of vertically and/or non-vertically dipping cracks. Most of the stations we have analyzed so far showed just one chief polarization direction (Figure 3). The recording of a single prevalent polarization may in general be accounted for by anisotropic effects due to parallel vertical cracks. In this case, the chief polarization orientation is parallel to the strike of the main crack system in the neighborhood of the station. Station P03, however, showed two almost equally dominant polarization directions, which may provide important clues on the geometry of subsurface fractures and should not be regarded as scattering noise, especially if their distribution fits particular azimuthally dependent patterns.

In addition to the trial-and-error process described above, a more self-consistent algorithm was developed for inverting the measurements of polarizations and time delays of split shear waves. Such a multi-response (φ and δt) inversion problem as above can be reduced to two connected single-response processes due to the following three features of the shear-wave splitting data. 1) Either the polarization or the time delay dataset is mathematically adequate by itself to invert for fractures. 2) Polarization data are basically insensitive to the variations in crack density. 3) The measurement of time delays technically involves much more uncertainties than that of polarizations.

More specifically, crack strike and dip are mainly modeled from polarizations while crack density is modeled from delay times. In order to implement the inversion scheme, a 2-D model plane is defined in which the x -axis represents the crack strike and the y -axis the complement of the crack dip, both spanning the range from -90° to 90° . The root mean square of the residue functions (RMSRF) are computed at specific points in this plane (by default, these points lie on a $1^\circ \times 1^\circ$ resolution grid) and their distributions are visualized by contouring. According to the nonlinear least squares rule, the estimated crack model is inferred from the point where the absolute RMSRF minimum is located.

Preliminary Inversion Results

To model the effects of crack-related anisotropy (in terms of crack strike, dip and density) on shear-wave splitting behavior, the fractured medium is represented by an elastic continuum with anisotropic properties that reflect the crack's configuration. This representation applies to wavelengths that are significantly longer than individual crack dimensions. We use the elastic stiffness proposed by MacBeth (1999) for Transverse Isotropic (TI) conditions, which includes a first order perturbation to the isotropic elastic constants, to simulate the general 3-D mechanical properties of the fractured solid. By evaluating the eigenvalues and eigenvectors of the corresponding Christoffel matrix, which depend on the medium stiffness and direction of wave propagation, synthetic fast shear-wave polarizations, shear-wave phase velocities, and associated differential time delays can be calculated for prescribed transversely isotropic models (Babuska and Cara, 1991; Tsvankin, 2001).

The preliminary inversion results for crack strike, crack dip, and crack density using the measured fast shear-wave polarization directions and differential time delays from the five selected seismic stations in Krafla geothermal field are listed briefly in Table 1. Compared to the results of other stations, the shallow dip angle and high crack density inverted for P04 may indicate that the fracture model of a single set of vertical or non-vertically dipping cracks is probably not appropriate in this case. All the other inversion results are generally consistent with the assumption of the single set model in terms of their steep dip angles and relatively low crack densities. The crack strikes for stations P13 and P23 are close to E-W direction while at station P10 the strike is almost in N-S direction. These results again show that there may exist two different systems of fractures in Krafla, which is not very surprising. The fitting between the observed and theoretical fast shear-wave polarizations for station P13 is plotted in equal-area projection and shown in Figure 5. The fitting is generally good although there are still some cases in

which the observed and theoretical polarizations are nearly perpendicular to each other. These perpendicular cases may provide important clues to the possible relation between the subsurface crack systems and changes in water pressure as will be discussed in the following section.

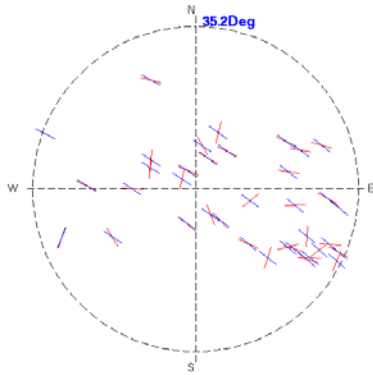


Figure 5. The fitting between the observed and theoretical fast shear-wave polarizations for station P13 plotted in equal-area projection. The red line segments are observed and blue ones are theoretical.

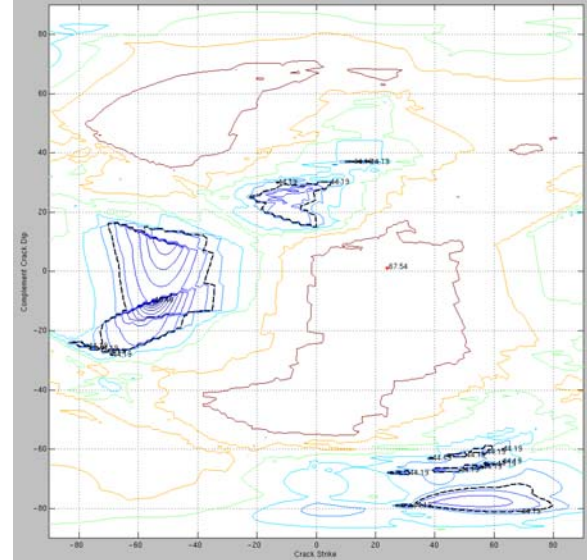
Shown in Figure 6 are the residual contours computed for stations P13 and P23 for the purpose of determining the crack strike, crack dip and crack density corresponding to the minimum of residuals in fast shear-wave polarizations and/or differential time delays. It is anticipated that the resulting pairs of crack strike and crack dip inferred from the global RMSRF minima in both residual contours are the same or very close to each other as the case for station P23 is, but actually the results from the two contours may be quite different from each other, probably because, as stated before, the measurement of time delays technically involves much more uncertainties than that of polarizations. For this reason we have listed in Table 1 only the results inverted for using the trial-and-error method for each analyzed station.

Table 1. Inversion results of crack parameters with trial-and-error method.

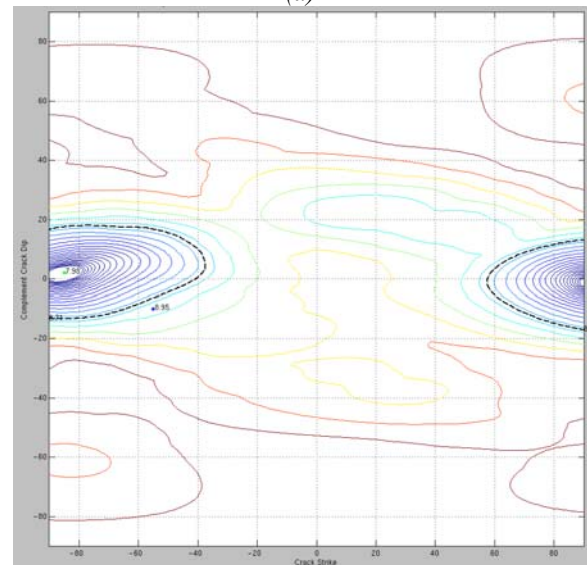
Station ID	Crack Strike (Degree)	Crack Dip (Degree)	Crack Density
P03	82	-55	0.065
P04	71	-16	0.072
P10	-1	73	0.027
P13	-55	80	0.024
P23	-73	-74	0.027

DISCUSSION AND CONCLUSION

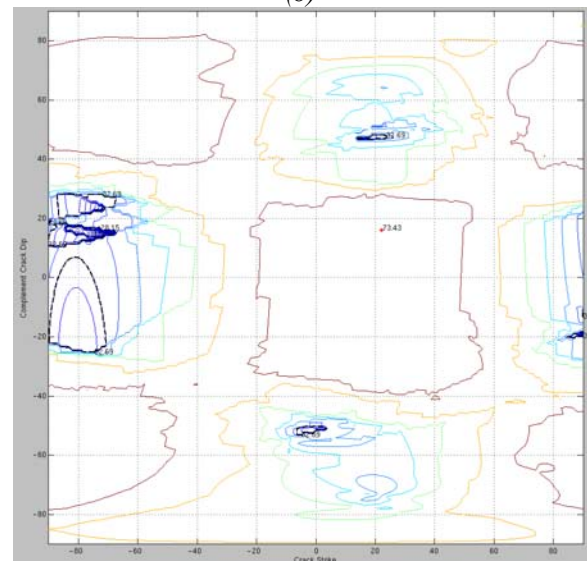
A 20-station, 3-component digital seismic array was deployed around the Krafla geothermal field in Iceland in July and August of 2004, and the seismic



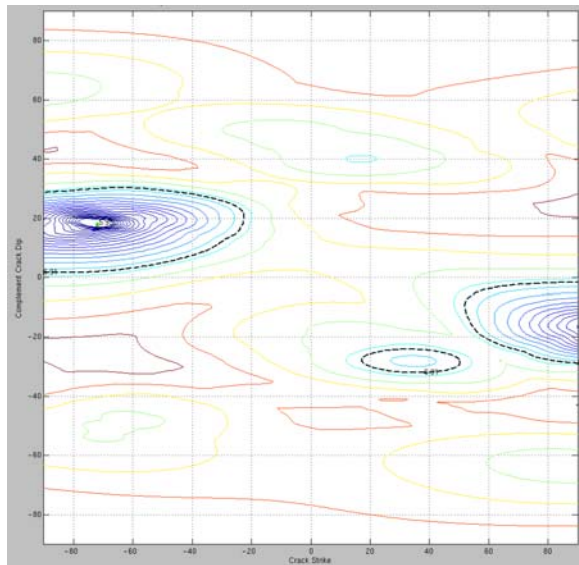
(a)



(b)



(c)



(d)

Figure 6. Residual contours computed for stations P13 and P23 to invert for the crack strike, dip and density. (a) The global minimum of polarization residual for P13 is located at strike=-55° and dip=80°. (b) The global minimum of time delay residual for P13 is located somewhere else. (c) The global minimum of polarization residual for P23 is located at strike=-73° and dip=-74°. (d) The global minimum of time delay residual for P23 is located at the same pair of strike and dip as in (c).

data set we have collected there is unique. We have also monitored the injection stoppage and resumption and collected data at a sampling rate of 500 sps which is high enough to allow detection of even the smallest variations in crack density and the possible flow of fluids through the crack system. The seismicity in the Krafla field is not very high (3-4 usable events per day), with most epicenters located along an E-W oriented belt north of the injection well and typical focal depths shallower than 4 km.

There is clear evidence of shear-wave splitting in the seismic data. In addition to the observed prevalence of a crack system oriented in approximately N-S direction which is consistent with the anticipated direction of major fractures in the area, fast shear-wave polarization directions along a general E-W direction are also persistent, more than along any other direction as shown in stations P13 and P23. The highest intensity of cracking detected so far occurs along N70-80E directions (stations P03 and P04), and most cracks have a relatively deep dipping angle.

In order to investigate the response of subsurface crack systems to changes in fluid pressure inside the medium, the injection in well K-26 was stopped for ten days before resumed on July 26. There is

preliminary evidence that the injection modifies the observed crack polarizations in some areas. In Figure 5 we can see that except for the prevalent nearly E-W polarizations, there are still a few cases whose polarizations are close to N-S. Two of these “irregular” events have been identified as shortly after the stoppage of injection and five as after the resumption. This may imply that changes in water pressure have to some extent changed the effects of the cracks on the polarization angles of the fast shear-wave propagating through them.

In hindsight it became clear that most of the 20 stations of the array had been placed in optimal locations to retrieve seismic information for fracture characterization. We expect that with a permanent array at these locations the field can be accurately monitored.

REFERENCES

- Babuska, V. and Cara, M. (1991), *Seismic Anisotropy in the Earth*, Modern Approaches in Geophysics, Vol. 10, pp. 217, Kluwer Academic Publishers, The Netherlands.
- Booth, D.C. and Crampin, S. (1985), “Shear-wave polarizations on a curved wavefront at an isotropic free-surface”, *Geophys. J. Roy. Astr. Soc.*, **83**, 31-45.
- Brandsdottir, B., Menke, W., Einarsson, P., White, R.S., and Staples, R.K. (1997), “Faroe-Iceland Ridge Experiment 2. Crustal structure of the Krafla central volcano”, *J. Geophys. Res.*, **102**, 7867-7886.
- Einarsson, P. (1978), “S-wave shadows in the Krafla caldera in NE-Iceland, evidence for a magma chamber in the crust”, *Bull. Volcanol.*, **41**, 1-9.
- Crampin, S. (1987), “Geological and industrial implications of extensive dilatancy anisotropy”, *Nature*, **328**, 491-496.
- Crampin, S., Booth, D.C., Krasnova, M.A., Chesnokov, E.M., Maximov, A.B., and Tarasov, N.T. (1986), “Shear-wave polarizations in the Peter the First range indicating crack-induced anisotropy in a thrust-fault regime”, *Geophys. J. Roy. Astr. Soc.*, **84**, 401-412.
- Crampin, S. and Lovell, J.H. (1991), “A decade of shear-wave splitting in the Earth’s crust: What does it mean? What use can we make of it? And what should we do next?” *Geophys. J. Int.*, **107**, 387-407.
- Hudson, J.A. (1981), “Wave speeds and attenuation of elastic waves in materials containing cracks”, *Geophys. J. Roy. Astr. Soc.*, **64**, 133-150.

Peacock, S., Crampin, S., Booth, D.C., and Fletcher, J.B. (1988), "Shear-wave splitting in the Anza seismic gap, southern California: temporal variations as possible precursors", *J. Geophys. Res.*, **193**, 3339-3356.

Tryggvason, E. (1986), "Multiple magma reservoirs in a rift zone volcano: Ground deformation and magma transport during the September 1984 eruption of Krafla, Iceland", *J. Volcanol. Geothermal Res.*, **28**, 1-44.

Tsvankin (2001), *Seismic Signature and Analysis of Reflection Data in Anisotropic Media, Handbook of Geophysical Exploration, Section I, Seismic Exploration*, 1st edn, Vol. 29, pp. 436, Pergamon, Amsterdam, New York.

Yang, M. (2003), *Inversion of shear-wave splitting data in geothermal reservoirs*, Master's thesis, University of North Carolina, Chapel Hill, NC.